J Solid State Electrochem (2012) 16:723–729
DOI 10.1007/s10008-011-1417-5

ORIGINAL PAPER

Electrochemical properties of freestanding TiO_2 nanotube membranes annealed in Ar for lithium anode material

Yue Wang · Suqin Liu · Kelong Huang · Dong Fang · Shuxin Zhuang

Received: 11 February 2011 / Revised: 19 April 2011 / Accepted: 23 April 2011 / Published online: 12 May 2011

Abstract Freestanding and highly ordered TiO_2 nanotube membranes were prepared via anodization and annealed at 450, 600, and 800 °C in air and Ar, respectively. Based on the results of XRD and SEM, the membranes annealed in Ar and air possessed different morphology and crystalline phases. Compared with the sample annealed in air, a trace amount of carbon on TiO_2 membrane annealed in Ar was detected by EDS spectrum. Electrochemical measurements showed that TiO_2 membrane annealed in Ar exhibited better discharge capacity and cyclic stability. The noticeably improved electrochemical performances were attributed to the presence of carbon which enhanced the surface electronic conductivity, the crystalline transformation, and the appropriate morphology, such as large pore, thin wall, and well tube structure.

Keywords Lithium ion batteries · TiO_2 nanotube membrane · Anodization · Ar

Introduction

TiO_2 has been considered as an alternative anode material in lithium ion batteries due to its high Li^+ intercalation voltage plateau and relatively stable cycle performance [1–3]. And the TiO_2 nanotube exhibiting relatively larger surface area and shorter diffusion path for Li^+ intercalation than other nanostructures is an excellent candidate as a stable electrode in Li^+ batteries [4]. It can be prepared via anodization [5] and hydrothermal methods [1, 6]. However, TiO_2 nanotubes grown from the hydrothermal method are random with varied orientations. Anodization is a relatively convenient and effective technique to fabricate highly ordered vertically oriented TiO_2 nanotube arrays on Ti substrates [7]. In addition, the structure parameters such as the diameter and length of nanotubes can be easily controlled during anodization [8]. Well-oriented TiO_2 nanotubes produced by anodization can facilitate the close contact between nanotubes and electrolyte, which favor electron and Li^+ transfer. Thus, it could be a potentially promising Li^+ intercalation host [9–12].

However, the low Li^+ and electronic conductivity of TiO_2 are the main obstacles for their practical applications. Some studies about metals such as Ag and Sn modifying TiO_2 nanotube anode material to improve the surface electronic conductivity have been reported [13, 14] while, the established coating techniques were often complicated and the uniformity of the coating was another challenge [15]. Thermal annealing in reducing or inert gas has been actively studied on many materials [16–18]. Liu et al. [17] reported that annealing TiO_2 nanotube arrays in reducing gas CO resulted in improved Li^+ intercalation properties and enhanced the electronic conductivity due to the surface defects and oxygen vacancies. The results indicated that thermal annealing in reducing or inert gas could be a viable method to improve the electrochemical properties. Following this idea, the electrochemical properties of anodization derived TiO_2 nanotubes annealed in air and in inert gasses have been compared. And, it was found that TiO_2 nanotubes could possess different microstructure and crystallinity when annealed at different temperatures, significantly influencing the Li^+ intercalation properties [4, 16]. Moreover, previous researches are undertaken by using the nanotubes on Ti substrates. The weight of Ti substrates may lead to low energy density. And the

Y. Wang · S. Liu (✉) · K. Huang · D. Fang · S. Zhuang
College of Chemistry and Chemical Engineering,
Central South University,
Changsha 410083, China
e-mail: sqliu2003@126.com

application of TiO_2 nanotubes on the substrates would be limited. In the present paper, we synthesized self-organized TiO_2 nanotube arrays via anodization and obtained the freestanding TiO_2 membranes. Then the membranes were annealed at different temperatures in air and Ar. Finally, the relationship between the annealing atmosphere and temperature, morphology, crystalline phase, and electrochemical properties was investigated.

Experiment

Materials preparation

TiO_2 nanotube arrays were synthesized by the anodization method. The samples of Ti foil (0.30 mm thick, 99.5% purity) were sonicated in acetone to remove organic dirt and then rinsed with distilled water and dried in air.

The anodization was performed in a two-electrode configuration under a constant voltage of 50 V at room temperature. A Ti foil was used as anodic electrode while Pt was used as cathodic electrode. The distance between the two electrodes was maintained at 10 mm. The electrolyte in this process was 0.25 wt.% NH_4F dissolved in a mixture of ethylene glycol and deionized water. The anodization period was 24 h. After that, the whole sample was transferred into a mixture of ethanol and deionized water (9:1 in volume) and sonicated fiercely for several minutes. The TiO_2 membrane will be detached from the Ti substrate during the ultrasonication. The membrane was rinsed with ethanol and then calcined at temperatures of 450, 600, and 800 °C under respective dry gas flow of air and Ar with a heating rate of 10 °C/min and dwelled at the maximum temperature for 3 h.

Characterization

X-ray diffraction (XRD) measurement was carried on a RigaKu D/max2550VB$^+$ 18 kW using graphite-monochromatized Cu Kα radiation (40 kV, 250 mA). The morphology of the samples was observed by a JSM-6360-LV scanning electron microscopy (SEM) equipped with an energy dispersive spectrometer (EDS). Elemental analysis was used to determine the precise carbon content in samples by C-S600 infrared carbon sulfur analyzer.

Electrochemical measurements

The electrochemical performances of as-prepared TiO_2 membrane were evaluated using a CR2016 coin cell, in which TiO_2 membrane was used as working electrode and a Li foil as the counter electrode. The electrolyte was 1 M $LiPF_6$ dissolved in a mixture of ethylene carbonate, dimethyl carbonate, and methyl-ethyl carbonate with a volume ratio of 1:1:1. For these experiments, no additives such as polyvinylidene fluoride acting as binder agent and acetylene black acting as conductive agent were used. Assembling of the cells was performed in an argon-filled glove box (Mbraun, Unilab, Germany). The cells were galvanostatically charged and discharged between 1.0 and 2.5 V on the electrochemical test instrument (CT2001A, Wuhan Land Electronic Co. Ltd., China). Cyclic voltammetry measurements were performed using electrochemical workstation (Shanghai Chenhua Instrument Co. Ltd., China) at a scan rate of 0.1 mV/s between 1.0 and 2.5 V. Electrochemical impedance spectroscopy was recorded by the ZAHNER-IM6 electrochemical workstation (Germany) over the frequency range from 100 kHz to 0.01 Hz with an amplitude of 5 mV. All potentials are cited in this paper with respect to the reference Li^+/Li.

Results and discussion

SEM images of the TiO_2 membranes after annealing in air and Ar are shown in Fig. 1. As Fig. 1a–c show, the TiO_2 membrane remains basically nanotubes structure with inner diameter of about 85 nm and smooth surface of the tube wall after annealing at 450 °C in air. However, there are some significant changes in the open pore size as well as the surface morphology after annealing at 600 °C. And the pore size is reduced and the nanotube wall thickness is increased. Moreover, the surface of TiO_2 nanotube arrays turns rough with many small particles. The size of these particles tends to become larger as the calcination temperature increases. When annealed at 800 °C, the nanotube changes into particles along the long tube axis. And the decrease of pore size as well as the increase of wall thickness is more pronounced. Figure 1d–f show general views of TiO_2 membranes after annealing at 450, 600, and 800 °C in Ar for 3 h. The morphology changes of nanotubes are relatively slow and the particles on the wall are only found at 800 °C. This indicates that annealing in Ar results in greater preservation of the structure of nanotube than in air. A trace amount of carbon was found in EDS spectrum of TiO_2 membrane annealed in Ar at 450 °C (Fig. 2b), which was obtained by heating organic matter of electrolyte in the absence of O_2. Furthermore, in order to determine the precise carbon contents in these samples annealed in Ar at various temperatures, the carbon elemental analysis was conducted. The results showed that the carbon contents of the samples annealed at 450, 600, and 800 °C in Ar were 5.122, 4.943, and 4.852 wt.%, respectively. It indicated that the carbon content in these samples almost kept constant with the calcination temperature increasing.

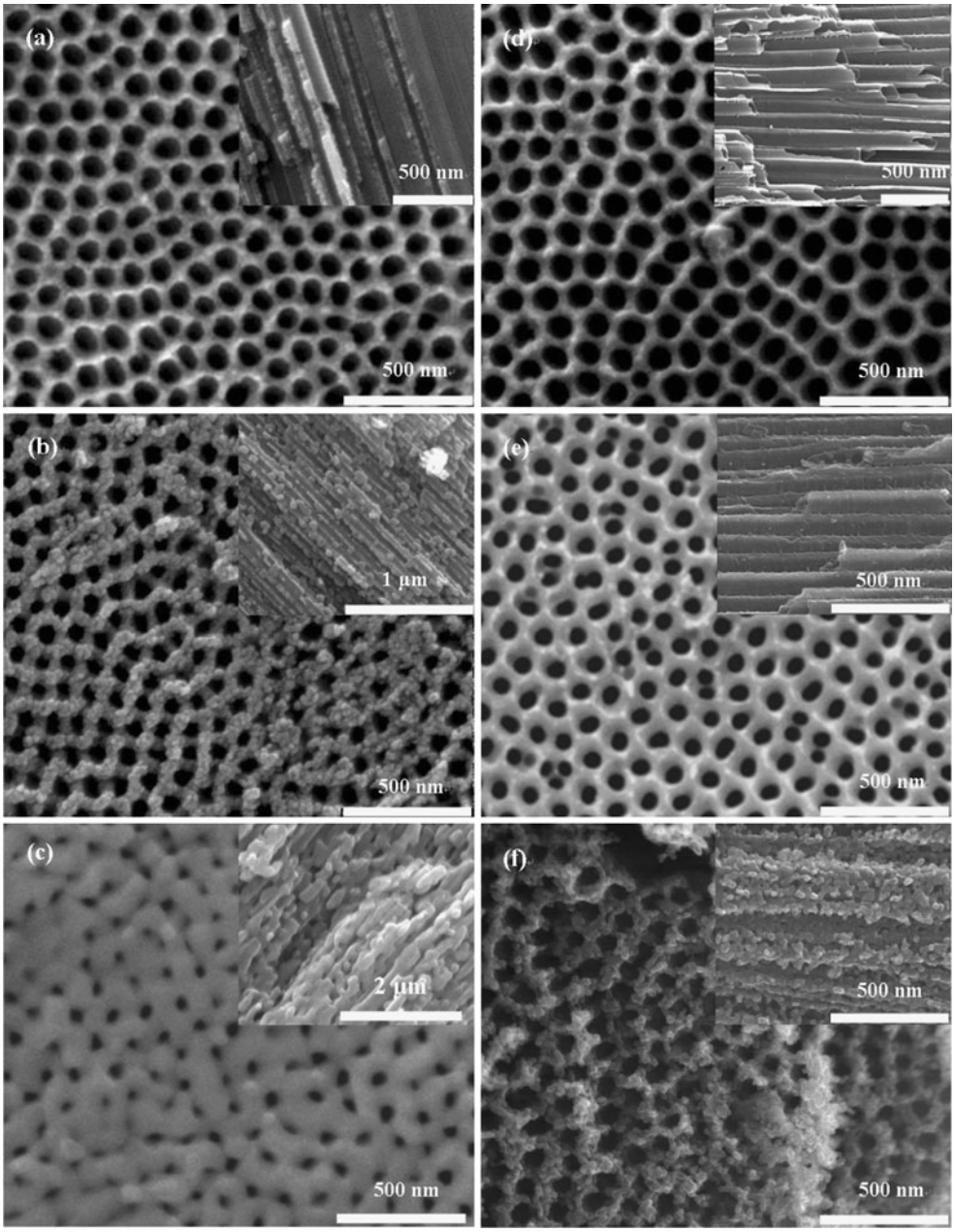

Fig. 1 SEM images of the top surface and cross-section of TiO_2 membranes annealed in air or Ar at different temperatures: **a** 450 °C, **b** 600 °C, **c** 800 °C, in air and **d** 450 °C, **e** 600 °C, **f** 800 °C in Ar for 3 h

The XRD patterns of products are shown in Fig. 3. The crystal phases of TiO_2 membranes annealed at 450, 600, and 800 °C in air for 3 h are identified to be anatase phase. No rutile phase is detected. The peaks at scattering angles of 25.18°, 37.78°, 48.00°, 53.89°, 54.99°, 62.57°, 68.68°, 70.15°, and 75.01° correspond to the reflections from the (101), (004), (200), (105), (211), (204), (116), (220), and (215) crystal planes of anatase TiO_2, respectively. XRD patterns of the specimens annealed in Ar are given in Fig. 3b. The pure anatase phase is obtained only for the as-prepared TiO_2 nanotube membranes calcinated at 450 °C in Ar. However, after annealing at 600 °C and 800 °C, rutile phase appears and coexists with anatase phase. Our results demonstrate that the crystalline transformation is easier to occur when annealed in Ar condition.

The anatase-to-rutile transformation may be conducted at a wide range of temperatures 400–1,100 °C, though normally it takes place at about 800–850 °C [19]. And it is influenced by material preparation procedure, particle size and shape, calcination temperature and atmosphere, and dopants [19–21]. It has been found that oxygen vacancies could accelerate the anatase-to-rutile transformation and lower the transformation temperature [20–22]. Zhang et al. [23] also pointed out that the phase transition was promotive in CO gas rather than in O_2. Therefore, these studies all indicate that annealing in dry Ar or in CO

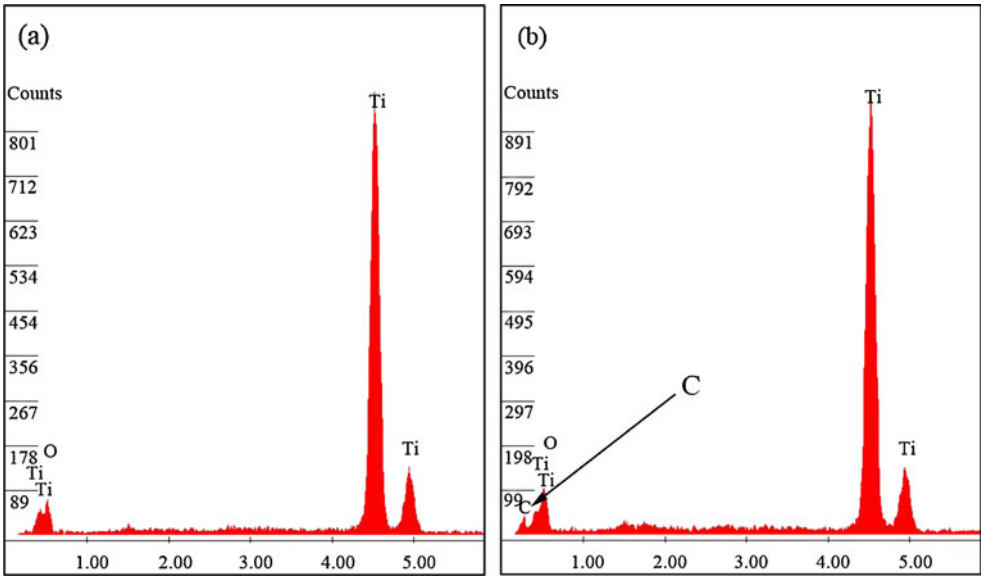

Fig. 2 EDS spectra of TiO_2 membranes annealed at 450 °C **a** in air and **b** in Ar

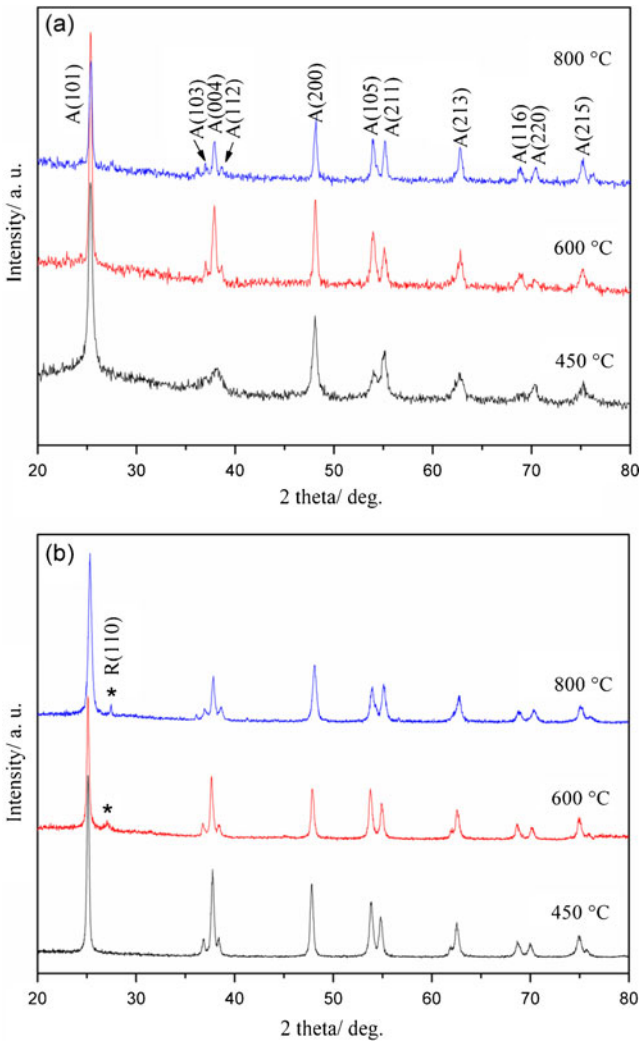

Fig. 3 XRD spectra of TiO_2 membranes annealed **a** in air and **b** in Ar

generate more oxygen vacancies in TiO_2 than annealing in air or O_2. Such oxygen vacancies benefit the anatase-to-rutile transformation.

Charge–discharge measurement was performed to examine the electrochemical behavior of the TiO_2 membranes as lithium anode materials. The initial discharge/charge curves for TiO_2 membranes annealed in air and Ar at 25 mA/g in the potential range of 1.0–2.5 V are shown in Fig. 4a. As can be seen, all the samples exhibit one discharge plateaus around 1.77 V and corresponding a charge plateaus around 1.9 V, which indicates that the insertion and extraction of Li^+ occur in one stage [6]. TiO_2 membranes annealed in air at 450, 600, and 800 °C deliver the discharge capacities of 209, 195.1, and 163.3 mAh/g, respectively. For TiO_2 membranes annealed in Ar, the corresponding discharge capacities are 227.9, 223.4, and 186.9 mAh/g, respectively. Apparently, the initial discharge capacity of TiO_2 membranes annealed in Ar is much higher than that annealed in air.

The cyclic stability of the TiO_2 membranes annealed in air and Ar for Li^+ intercalation was measured at a current density of 25 mA/g and shown in Fig. 4b. It is observed that TiO_2 membranes annealed in Ar possess better performance than those of annealed in air. At 450 °C, the specimen annealed in Ar exhibits excellent cyclic stability over long-term cycles with the capacity retention of 86.4% for the first 50 cycles. For the TiO_2 membrane annealed in air at the same temperature, the capacity retention of the first 50 cycles is 75.8%. Comparing the discharge capacities of the TiO_2 membranes annealed at different temperatures in air and Ar (Fig. 4b), it is clear that the reversible capacities and capacity retention rates have a tendency to decrease with the increasing of calcination temperature. However, the Li^+ intercalation capacity of the TiO_2 membranes annealed in Ar is always higher than that

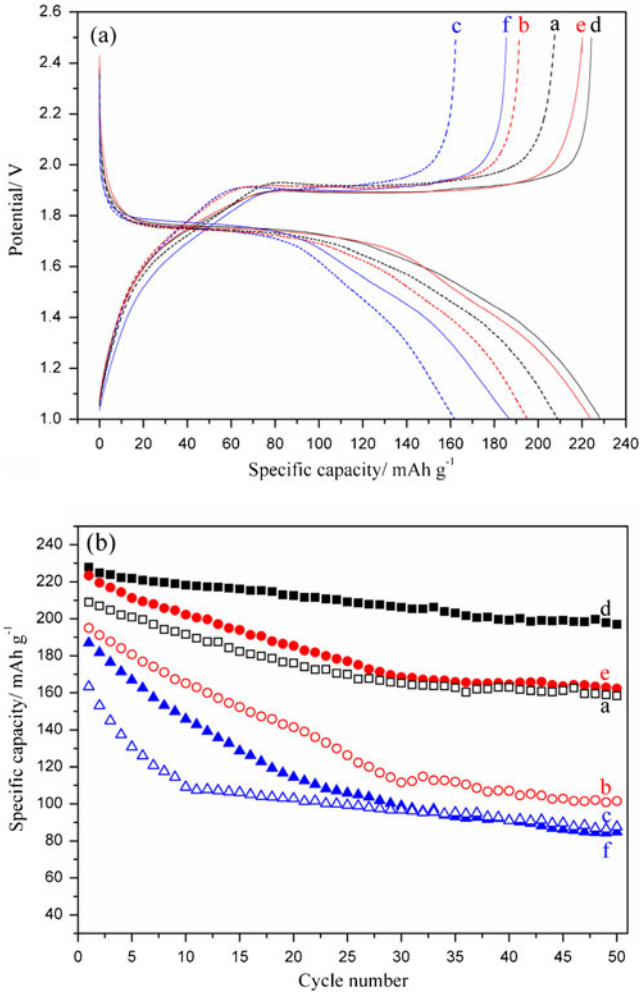

Fig. 4 **a** Initial charge and discharge curves. **b** Cycle performance of TiO_2 membranes at 25 mA/g between 2.5 and 1 V: *a*, *b*, *c* representing TiO_2 membranes annealed at 450 °C, 600 °C and 800 °C in air, while *d*, *e*, *f* being 450 °C, 600 °C, 800 °C in Ar, respectively

annealed in air at the same temperature. When annealed at 800 °C, the capacities of both the samples faded drastically and were below 90 mAh/g after 50 cycles. The reason leading to higher Li^+ intercalation capacities of the TiO_2 membranes annealed in Ar is most likely due to the change of crystalline phase and nanotube structures [16, 24]. According to the XRD spectra, after annealing at 600 °C and 800 °C in Ar, rutile phase appears and coexists with anatase phase. Some researchers reported that rutile nanomaterials not only had better electrochemical characteristics in terms of rate performance and capacity than micrometer-sized rutile but also the values even exceeded those of anatase of comparable size [25, 26]. SEM images also reveal that after annealed in Ar, the pore diameter shrinked slowly and the wall thickness is thinner than those of the membrane annealed in air at the same temperature. The discharge capability of TiO_2 membrane is strongly dependent on these morphological features [9, 16, 27]. Since the big pores favor the penetration of electrolyte and the more active materials can be utilized. Meanwhile, the big pores benefit Li^+ to get into the interior of the membrane, whereas the thin walls decrease the solid-phase diffusion length of Li^+ in active materials and the resulting capacity increases. In addition, it can be seen that the particles appeared on the tube wall grow up as the calcination temperature increases and the particle in air is larger than that in Ar. Kang et al. [28] found that the smaller particle size was achieved, the greater Li^+ insertion capability was obtained. Because the smaller the particle size is, the higher the surface area is and hence, the greater the interfacial area of contact between the electrode and electrolyte is. These factors certainly permit an apparently higher amount of Li^+ flux through the electrode/electrolyte interface [29]. While at 800 °C, the particles swell terribly in the two atmospheres and are like strings of beads which cause a blockage. That may be the reason for poor electrochemical performance of both the TiO_2 membranes annealed at 800 °C in Ar and air.

The relationship between cycling performance and the different current density for both TiO_2 membranes annealed in air and Ar at 450 °C is shown in Fig. 5. As the current density increasing, the discharge capacity decreases due to charge accumulation and polarization [17, 30]. While, the degeneration rate of specific discharge capacities for the TiO_2 membrane annealed in Ar is much lower than that annealed in air when the current density increases. It is clear from Fig. 5 that the TiO_2 membrane annealed in Ar possesses much higher intercalation capacities, approximately double of that of TiO_2 membrane annealed in air at 250 mA/g and three times at 500 mA/g. The explanations of the excellent high-rate performance are below. Owing to the less shrinkage in pore size, the TiO_2 membranes annealed in Ar has larger specific surface area, which

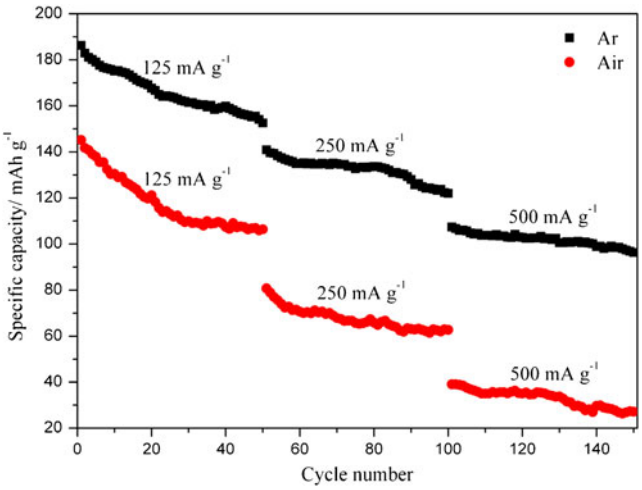

Fig. 5 Cycle performance of TiO_2 membranes annealed in air and Ar at 450 °C at different current density

decreases the current density per unit surface area of the electrodes, thus decreasing the electrochemical polarization [11]. Furthermore, compared with Fig. 2a, carbon element exists in the membrane annealed in Ar (as shown in Fig. 2b) which improves the surface electronic conductivity and makes the Li^+ transfer into TiO_2 nanotubes structure more easily. And the oxygen vacancies in TiO_2 created by annealing in Ar may also contribute to enhance charge–transfer conductivity [17, 18].

Figure 6 shows the initial cyclic voltammograms of TiO_2 membrane annealed in air and Ar at 450 °C under the identical conditions. For membrane annealed in air, one cathodic peak centered at 2.16 V was identified and the corresponding anodic peak at 1.63 V was observed. Appearance of redox peaks indicates the reversible Li^+ intercalation and de-intercalation in solid phase. For the CV curve of TiO_2 membrane annealed in Ar, a pair of cathodic/anodic peaks located at 1.75 and 2.01 V, respectively, and the potential separation between anodic peak and cathodic peak was 0.26 V, lower than that of the sample annealed in air (0.48 V). This reduction of interval in peak voltages indicated better reversibility of Li^+ intercalation and de-intercalation. What is more, the peak current of the TiO_2 membrane annealed in Ar was much bigger than that of annealed in air, indicating higher Li^+ diffusion coefficient of the membrane annealed in Ar.

In order to further understand the reason for better electrochemical performance of TiO_2 membrane annealed in Ar, Nyquist plots of TiO_2 membranes annealed in air and Ar at 450 °C are recorded at different discharged states. As shown in Fig. 7a, all plots possess a semicircle at the high-to-medium frequency range and a sloping line at low frequency. The equivalent circuit for these cell systems is presented in Fig. 7b [13]. The R_s component stands for bulk resistance of

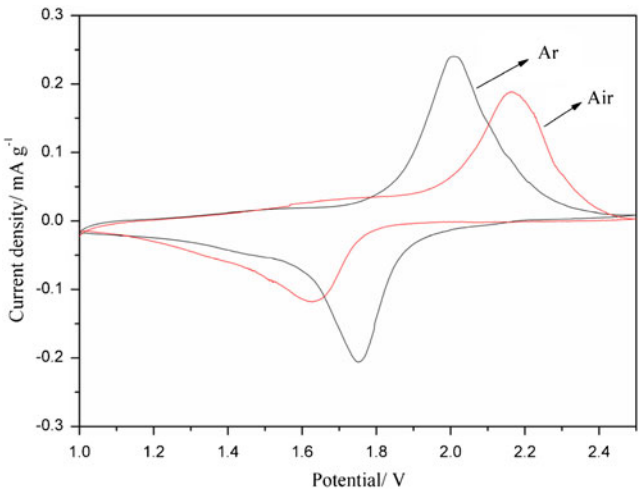

Fig. 6 Cyclic voltammograms of TiO_2 membranes annealed in air and Ar at 450 °C with a scan rate of 0.1 mV/s

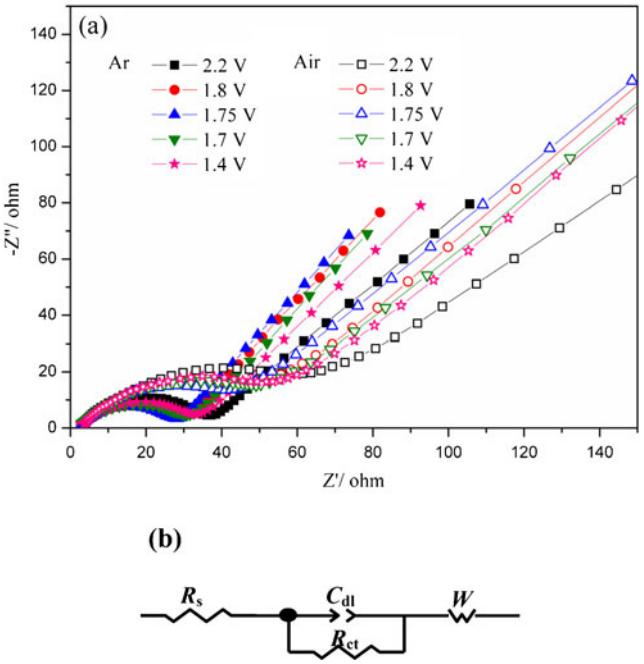

Fig. 7 **a** Nyquist plots of TiO_2 membranes annealed in air and Ar at 450 °C at different potential. **b** The equivalent circuit used to fit the electrochemical impedance spectroscopy

the electrode [31]. R_{ct} and C_{dl} represent charge–transfer resistance and double-layer capacitance, respectively, corresponding to the high-frequency semicircle. And the W is Warburg impedance representing the diffusion process of Li^+ inside the electrode, which is indicated by an inclined straight line. As Fig. 7a show, the semicircles decrease slightly and then increase from 2.2 to 1.4 V in the discharge mode. The charge transfer resistance is proportional to the diameter of semicircle in high-frequency region, which reaches the minimum value around the plateau voltage. That is in consistent with the reported behavior of nanotube electrodes [32, 33]. And the diameter of semicircles for TiO_2 membrane annealed in Ar are all obviously smaller than those of the membrane annealed in air, indicating that the charge transfer is more favorable on the electrode annealed in Ar. The reduced resistance in the high frequency of TiO_2 membrane annealed in Ar could be ascribed to the carbon and the oxygen vacancies created by annealing in Ar, improving the surface electronic conductivity.

Conclusions

Freestanding TiO_2 nanotube membranes were fabricated and annealed in air and Ar at various temperatures. The TiO_2 membrane annealed at 450 °C in Ar exhibited the best electrochemical property with an initial discharge capacity of 227.9 mAh/g and a capacity retention of 86.4% for the first

50 cycles at a current density of 25 mA/g. Annealing in Ar significantly improved the reversible capacity and the cycling stability. The good electrochemical performances were attributed to the carbon detected by EDS, the crystalline transformation, and the desirable morphology, such as large pore, thin wall, and well tube structure. Therefore, the predominant electrochemical performances of the TiO_2 membrane annealed at 450 °C in Ar make it greatly promising for the application of lithium anode material.

Acknowledgments This work was supported by National Science Foundation of China (No. 50972165) and Open-End Fund for the Valuable and Precision Instruments of Central South University.

References

1. Choi MG, Lee YG, Song SW, Kim KM (2010) Electrochim Acta 55:5975
2. Armstrong AR, Armstrong G, Canales J, Bruce PG (2005) J Power Sources 146:501
3. Sun CH, Yang XH, Chen JS, Li Z, Lou XW, Li CZ, Smith SC, Lu GQ, Yang HG (2010) Chem Commun 46:6129
4. Park SJ, Paek YK, Lee H, Kim YJ (2010) Electrochem Solid-State Lett 13:A85
5. Zhang XM, Huo F, Hu LS, Wu ZW, Chu PK (2010) J Am Ceram Soc 93:2771
6. He BL, Dong B, Li HL (2007) Electrochem Commun 9:425
7. Li SQ, Zhang GM, Guo DZ, Yu LG, Zhang W (2009) J Phys Chem C 113:12759
8. Xiao P, Garcia BB, Guo Q, Liu DW, Cao GZ (2007) Electrochem Commun 9:2441
9. Wei Z, Liu Z, Jiang RR, Bian CQ, Huang T, Yu AS (2010) J Solid State Electrochem 14:1045
10. Ortiz GF, Hanzu I, Djenizian T, Lavela P, Tirado JL, Knauth P (2009) Chem Mater 21:63
11. Fang HT, Liu M, Wang DW, Sun T, Guan DS, Li F, Zhou JG, Sham TK, Cheng HM (2009) Nanotechnol 20:225701
12. Ortiz GF, Hanzu I, Knauth P, Lavela P, Tirado JL, Djenizain T (2009) Electrochim Acta 54:4262
13. Fang D, Huang KL, Liu SQ, Li ZJ (2008) J Alloys Compd 464:L5
14. Kim HS, Kang SH, Chung YH, Sung YE (2010) Electrochem Solid-State Lett 13:A15
15. Fu LJ, Liu H, Li C, Wu YP, Rahm E, Holze R, Wu HQ (2006) Solid State Sci 8:113
16. Liu DW, Xiao P, Zhang YH, Garcia BB, Zhang QF, Guo Q, Champion R, Cao GZ (2008) J Phys Chem C 112:11175
17. Liu DW, Zhang YH, Xiao P, Garcia BB, Zhang QF, Zhou XY, Jeong YH, Cao GZ (2009) Electrochim Acta 54:6816
18. Liu DW, Liu YY, Garcia BB, Zhang QF, Pan AQ, Jeong YH, Cao GZ (2009) J Mater Chem 19:8789
19. Ratajska H (1992) J Therm Anal 38:2109
20. Gesenhues U (1997) Solid State Ionics 101:1171
21. Francisco MSP, Mastelaro VR (2002) Chem Mater 14:2514
22. Rath C, Mohanty P, Pandey AC, Mishra NC (2009) J Phys D Appl Phys 42:205101
23. Zhang YH, Xiao P, Zhou XY, Liu DW, Garcia BB, Cao GZ (2009) J Mater Chem 19:948
24. Wang Y, Takahashi K, Lee K, Cao GZ (2006) Adv Funct Mater 16:1133
25. Hu YS, Kienle L, Guo YG, Maier J (2006) J Adv Mater 18:1421
26. Wang DH, Choi DW, Yan ZG, Viswanathan VV, Nie ZM, Wang CM, Song YJ, Zhang JG, Liu J (2008) Chem Mater 20:3435
27. Yamada H, Yamato T, Moriguchi I, Kudo T (2004) Solid State Ionics 175:195
28. Kang JW, Kim DH, Mathew V, Lim JS, Gim JH, Kim J (2011) J Electrochem Soc 158:A59
29. Jiang CH, Wei MD, Qi ZM, Kudo T, Honma I, Zhou HS (2007) J Power Sources 166:239
30. Stephenson DE, Hartman EM, Harb JN, Wheeler DR (2007) J Electrochem Soc 154:A1146
31. Yoon SH, Kim HJ, Oh SM (2001) J Power Sources 94:68
32. Wang J, Zhou YK, Hu YY, O'Hayre R, Shao ZP (2011) J Phys Chem C 115:2529
33. Zhou YK, Cao L, Zhang FB, He BL, Li HL (2003) J Electrochem Soc 150:1246